Morphology of thin nanocomposite films of asymmetric diblock copolymer and magnetite

nanoparticles

Morphology of thin nanocomposite films of asymmetric diblock copolymer and magnetite nanoparticles

Valeria Lauter[1,3]**, Peter Müller-Buschbaum**[2]**, Hans Lauter**[1]
and Winfried Petry[2]

[1] Spallation Neutron Source, Neutron Scattering Science Division, Oak Ridge National
Laboratory, One Bethel Valley Road, Oak Ridge, TN 37831-6475, USA
[2] Technische Universität München, Physik-Department E13, Lehrstuhl für Funktionelle
Materialien, James-Franck-Straße 1, 85747 Garching, Germany

E-mail: lauterv@ornl.gov

Abstract

Thin self-assembled nanocomposite films of an asymmetric diblock copolymer and nanoparticles are fabricated. The morphologies of the films of the diblock copolymer poly(styrene-*block*-n-butyl methacrylate), P(Sd-*b*-BMA), with different volume fractions of large magnetite Fe_3O_4 nanoparticles are studied before and after annealing. Neutron reflectometry reveals remarkable evidence that confining asymmetric copolymer to a limit of two layers forces the film, after the annealing, to form a mixed cylindrical–lamellar two-layer structure. This complex morphology is very stable and is preserved after the incorporation of nanoparticles up to 10% volume fraction. The other striking result is that the monodispersed nanoparticles with affinity to the polystyrene (PS) domain and with a size of 10 nm, which is close to the size of the PS chains, are assembled by the diblock copolymer matrix, so the distribution of the nanoparticles is reduced solely to the PS domain of the film. Our studies demonstrate that for asymmetric block copolymers in thin film geometry the self-assembly is strongly influenced by the interfacial and surface energies of the blocks and substrate.

(Some figures in this article are in colour only in the electronic version)

1. Introduction

Thin polymer films with an ordered arrangement of polymer chains are used as matrices for new functional materials. The self-assembly of block copolymers into well-ordered structures due to microphase separation has attracted significant interest over the past few decades [1–5]. Confining the block copolymer to a thin film adds additional constraints on the final morphology due to an increased contribution of the substrate and surface effects [6]. As a result of this, the equilibrium behavior of block copolymers in thin films can be very different from that of bulk-like thick films [7–9]. The inner structure of the film and its surface pattern are influenced by the film confinement. As a consequence, a transition between perpendicular and parallel morphologies was predicted for thin

films with cylindrical diblock copolymer morphology for film thicknesses of a few repeat units [10]. The evolution of the vertical orientation of cylinders into a parallel one as a function of the thickness gradient was studied for triblock copolymer films [11]. A comparative study of the thin film behavior of symmetric and asymmetric diblock copolymers has shown hexagonal packing of the cylinders with in-plane distortions, which was interpreted as being a consequence of the non-integral packing in asymmetric films [12].

An especially attractive application of self-assembled block copolymer films is the formation of nanocomposite materials via inclusion of nanoparticles into the copolymer assembly [13–18]. In our previous pioneering studies [19–21] of highly organized self-assembled diblock copolymer–nanoparticle thin films, the nanocomposite films were designed using a template matrix formed from a symmetric diblock copolymer. These copolymers spontaneously self-assembled

---

[3] Author to whom any correspondence should be addressed.

into a regular lamellar structure during annealing [22–24]. By coating the nanoparticles with polymer chains of one particular type, we provided a control on the nanoparticle distribution within selected domains of the lamellar structure. Nanoparticles, having a selective affinity to one of the blocks, self-assembled within this block during annealing. This mechanism led to a spatially distributed ordered arrangement of the nanoparticles within the copolymer matrix [25].

For the asymmetric case, meaning diblock copolymers with two unequal block lengths, the cylindrical morphology in self-assembled block copolymers has received most attention during the past few years. Cylinder-forming diblock copolymer thin films demonstrate a rich variety of different microstructures [26] that deviate from those of the bulk material due to confinement and surface energy effects. Lamellae, perpendicular and parallel cylinders were experimentally observed [11, 12, 27, 28] and shown in computer simulations [29–31]. Meanwhile, there is a lot of activity as regards using these systems for new functional materials by incorporation of nanoparticles into copolymer matrices [32–35]. Although there have been attempts to use self-assembly and the affinity of the nanoparticles to one of the blocks of the diblock copolymer, the well-controlled placement of the nanoparticles is still problematic, because big nanoparticle clusters can be formed [36] or the morphology of the diblock copolymer matrix gets gradually lost [37].

In the present work we fabricated and studied the morphology of composite thin films of asymmetric P(Sd-*b*-BMA) diblock copolymer and large magnetite Fe_3O_4 nanoparticles with an average diameter of 10 nm. We fabricated samples containing 5% and 10% volume fractions of nanoparticles. The sample of pure P(Sd-*b*-BMA) film is investigated as well, and the parameters obtained are used as a reference to trace the details of the modification in the composite films with increasing concentration of the nanoparticles. The samples are studied before and after annealing. Neutron scattering was applied to study the complex internal and surface structure of the composite films. Due to the high contrast of the neutron scattering between the deuterated polystyrene (PS) and protonated PBMA domains, we detect that even before the annealing the internal structure of the films is not uniform. It shows a partial phase separation for the asymmetric films both with and without nanoparticles. Neutron reflectometry reveals that after annealing, the combined well-organized two-layer structure of cylindrical and lamellar domains is imprinted in the thin films and holds after the incorporation of the nanoparticles. This combined morphology is driven by confinement effects and the surface energies of different components of the copolymer. Further, we determine that the nanoparticles, being coated with the short PS chains [19–21], are constrained solely to being in the PS domains.

2. Experimental details

2.1. Sample preparation

Samples were prepared using poly(styrene-*block*-n-butyl methacrylate) asymmetric diblock copolymer, denoted

as P(Sd-*b*-nBMA), with a molecular weight M_w = 166 400 g mol^{-1} and a polydispersity M_w/M_n = 1.17. The polystyrene block was fully deuterated, and the molecular weights of the fractions of the copolymer were M_w (PSd) = 59 400 g mol^{-1} and M_w (PBMA) = 107 000 g mol^{-1}. The diblock copolymer material was prepared anionically and was obtained from Polymer Standard Service, Mainz.

Magnetite Fe_3O_4 nanoparticles were covered with short polystyrene chains from α-lithium polystyrene sulfonated as described previously [26]. The mean size of the nanoparticles as determined with light scattering was 10 nm with 20% variance. To prepare thin films, P(Sd-*b*-nBMA) and PS-coated nanoparticles were blended in a toluene solution with 5% and 10% volume fractions of the nanoparticles. In addition, a sample of pure P(Sd-*b*-nBMA) without nanoparticles was produced as a reference. The films were prepared on cleaned silicon (Si) substrates [38] by a spin-coating of either a pure copolymer or a copolymer–nanoparticle toluene solution. Annealing was performed in vacuum above the glass transition temperature at $T = 160\,°C$ for 18 h.

2.2. Atomic force microscopy

An atomic force microscope (AFM) was used for the surface characterization of the composite diblock copolymer/nanoparticle thin films before and after annealing. The AFM measurements were carried out with a Dimension 3100 AFM microscope and NanoScope IIIa system controller (Digital Instruments, Santa Barbara, CA). The cantilevers were made of Si, and the resonance frequencies were 150–190 kHz. The measurements were performed in tapping mode (oscillating contact mode) under ambient air conditions.

2.3. Neutron specular reflection and off-specular scattering

The neutron reflectometry experiments were performed at the magnetism reflectometer [39] at the Spallation Neutron Source at Oak Ridge National Laboratory (Oak Ridge) and at the reflectometer REMUR [40] at the Frank Laboratory of Neutron Physics (JINR, Dubna) using the time-of-flight method. A well-collimated neutron beam impinges on the sample surface at a glancing angle α_i and specularly reflects at an angle α_f, so $\alpha_i = \alpha_f$. In the time-of-flight method, neutrons of different wavelengths are sorted according to the time needed for going from the source to the detector, i.e. the neutrons are sorted by neutron wavelength. The data were recorded with a position-sensitive detector for a wide range of incoming and outgoing wavevectors k_i and k_f. The reflected and scattered intensities are normalized for the detector efficiency and for the intensity spectrum of the incident beam. The data are presented in a two-dimensional (2D) intensity map as a function of p_i and p_f, where $p_i = 2\pi \sin\alpha_i/\lambda$ and $p_f = 2\pi \sin\alpha_f/\lambda$ are the components perpendicular to the sample surface of the incoming and outgoing wavevectors, respectively (see figure 1). The specular reflectivities are extracted from these two-dimensional intensity maps as a function of the incident momentum transfer normal to the surface, $Q_z = p_i + p_f = 4\pi \sin\alpha_i/\lambda$ (see figures 2 and 3).
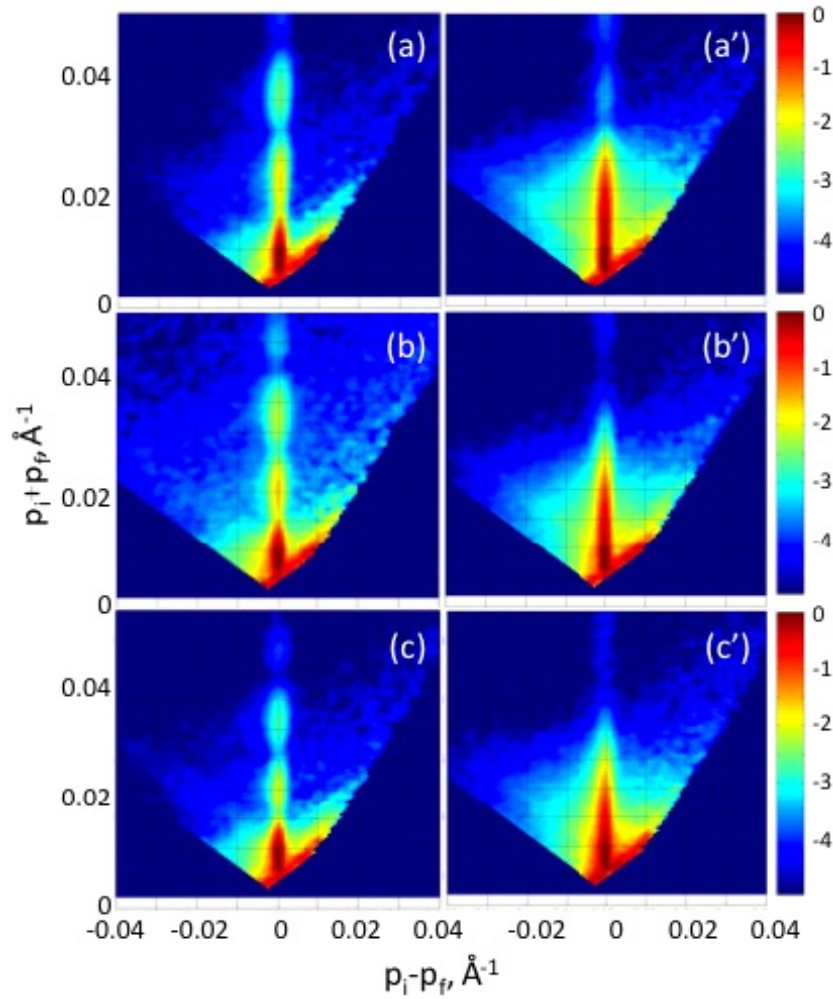
Figure 1. Experimental two-dimensional intensity maps from the non-annealed samples (left column) right after preparation of (a) the pure P(Sd-*b*-BMA) thin film and ((b), (c)) the copolymer film with incorporated Fe_3O_4 nanoparticles of 5% and 10%, respectively. The right-hand column represents the data from the samples as in (a), (b) and (c) but after annealing for 18 h at a temperature $T = 160\,^\circ C$. (a′) A pure copolymer film, (b′) copolymer film with 5% of nanoparticles and (c′) copolymer film with 10% of nanoparticles. p_i and p_f are the components perpendicular to the surface of the incoming and outgoing neutron wavevectors, respectively. The strong intensity along the line $p_i - p_f = 0$ corresponds to the specular reflection. The Yoneda scattering intensity spreads left and right from the specular line.

Neutron reflectometry experiments directly explore the depth profile of the films [41]. From the experimental data the neutron scattering length density (NSLD) is obtained. NSLD measures the Nb (with N being the atomic number density and b the scattering length averaged over a unit volume). The depth resolution in the present reflectometry experiments is 0.5 nm.

3. Results and discussion

3.1. Morphology of the composite films before annealing

The thin films of asymmetric diblock copolymers P(Sd-*b*-nBMA) without and with nanoparticles are first measured using neutron scattering before annealing. The results of the neutron scattering experiment are presented on the left panel in figure 1 as two-dimensional maps of the reflected and scattered intensities in coordinates of $p_i + p_f = Q_z$, with Q_z the momentum transfer of specular reflection, and $p_i - p_f$ the momentum transfer characterizing the off-specular

scattering [42]. The specular reflectivity runs along the line $p_i + p_f = Q_z$ at $p_i - p_f = 0$. The intensity and the pattern of the specular reflectivity are determined by the perpendicular structure of the film and the resolution function. The regular intensity oscillations are due to interference of neutrons reflected from the surface of the film and the film–substrate interface, and correspond to the total thickness of the film. The off-specular intensity originates from the surface and interfacial roughness and from the nanoparticles in the composite films. The small differences in the intensity maps for the non-annealed samples suggest that before the annealing the nanoparticles do not cause major modifications in the compositions of the films.

The specular reflectivity profiles extracted from the two-dimensional intensity maps are depicted in figure 2 (top) for non-annealed samples with volume fractions v_f of the nanoparticles taking values 0%, 5% and 10%.

The NSLD profiles obtained from the fit to the data are shown in figure 2. One might have expected that thin films
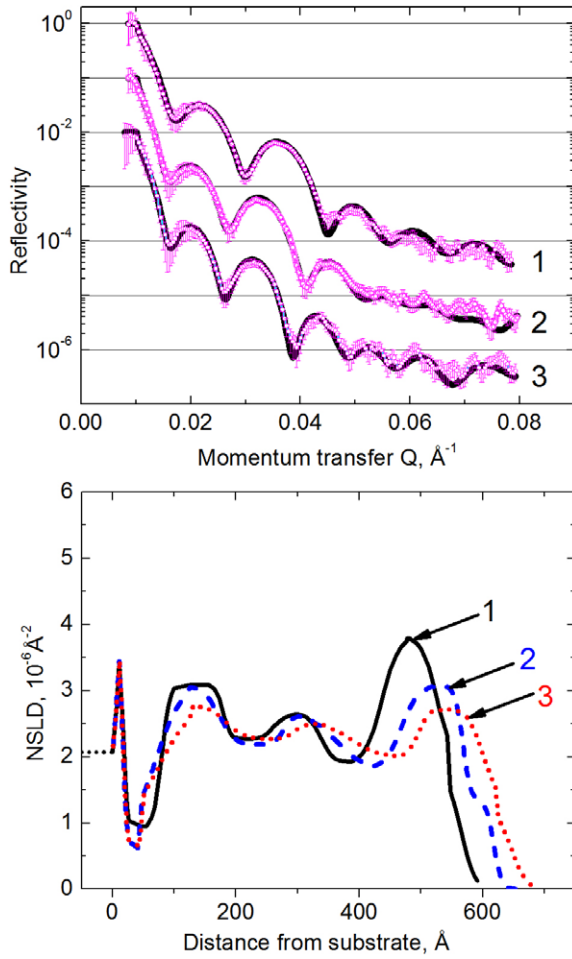
Figure 2. Top: experimental reflectivity profiles from non-annealed films of the pure block copolymer P(Sd-*b*-nBMA) (1) and the samples with 5% (2) and 10% (3) of nanoparticle volume fraction v_f, taken as vertical cuts along the line $p_i - p_f = 0$ from the left column two-dimensional maps in figure 1; the solid lines correspond to the fit to the data. Bottom: neutron scattering length density (NSLD) profile as a function of the distance from the substrate obtained from the model fit to the data, representing the depth profile of the structure of the non-annealed films with 0% (1), 5% (2) and 10% (3) of nanoparticles, and showing the increasing total thickness of the films and the modifications of the NSLD due to the presence of the nanoparticles. The narrow peak in the NSLD profile on the surface of the Si substrate corresponds to the natural SiO_2 thin layer.

Figure 3. Top: experimental reflectivity profiles from annealed films of the pure block copolymer P(Sd-*b*-nBMA) (1) and the samples with 5% (2) and 10% (3) of nanoparticle volume fraction v_f, taken as vertical cuts along the line $p_i - p_f = 0$ from the left column two-dimensional maps in figure 1; the solid lines correspond to the fit to the data. Bottom: neutron scattering length density profile as a function of the distance from the substrate obtained from the model fit to the data, showing the depth profile of the structure of the annealed films with 0% (1), 5% (2) and 10% (3) of nanoparticles, with increasing thickness and reducing NSLD of the PS layers due to the presence of the nanoparticles.

prepared by a spin-coating of a toluene blend of P(Sd-*b*-nBMA) with or without nanoparticles would form uniform films. However, the NSLD profile of the non-annealed films is not uniform. In the reference sample of pure P(Sd-*b*-nBMA) film, the PBMA blocks segregate toward the Si substrate due to the lower interfacial energies of PBMA and Si substrate, and are followed by a layer enriched with PS cylinders. This partially intermixed structure repeats from the substrate up to the surface of the film. A PBMA-enriched layer completes the film surface layer due to its lower (than for the PS) surface energy.

Such interaction driven interface enrichment might have evolved during the spin-coating due to the time necessary for deposition of the solution used.
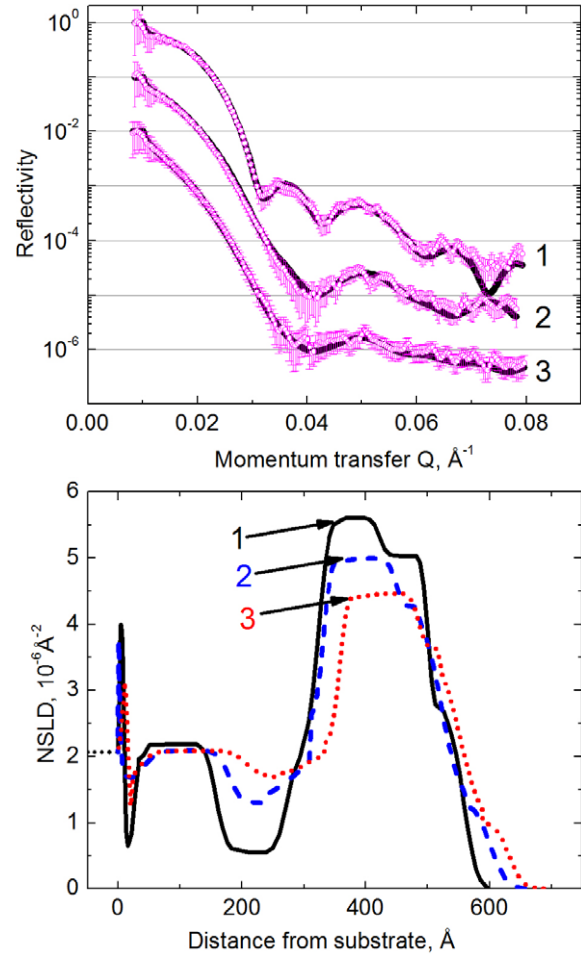
Thus our experimental results demonstrate that the film morphology results from a complex interplay of initial interactions and solvent evaporation of the whole film even at early stages of the spin-coating.

For the sample with 5% nanoparticles the morphology of the composite film is similar to that of the pure copolymer film, but with a reduced NSLD of the layers containing PS cylinders. Knowing that the average NSLD of the 10 nm nanoparticles coated with protonated PS chains of 1 nm is about 4.4×10^{-6} Å^{-2}, the addition of the nanoparticles to the PS-enriched parts of the film reduces the NSLD of this domain. This indicates that the PS-covered nanoparticles segregate toward the PS cylinders already in the as-prepared sample, during and after the spin-coating process. For the sample with 10% nanoparticles the morphology follows the same scenario.

The total film thickness increases with increasing fraction of the nanoparticles from 54.8 nm through 60 nm to 62.7 nm for films with 0%, 5% and 10% nanoparticles respectively.

3.2. Morphology of the composite films after annealing

After annealing of the samples, a well-ordered structure is constituted in these films. The neutron scattering experiment is repeated under the same conditions as for the as-prepared samples. The maps of the experimental data are shown in the right column in figure 1. The two-dimensional pattern of the off-specular scattering and the intensity along the reflectivity lines are very different from the ones obtained for the as-prepared samples.

The fit along the reflectivity lines (figure 3, top) reveals in the NSLD profile (figure 3, bottom) that the films have two very different morphological parts, one part located adjacent to the substrate and one part at the film surface. From the detailed analysis of the NSLD profile obtained for the reference sample with 0% nanoparticles, it follows that the Si substrate favors the PBMA block of the copolymer, so in the NSLD profile a layer with $Nb = 0.6 \times 10^{-6}$ Å^{-2} is formed, followed by a layer with $Nb = 2.26 \times 10^{-6}$ Å^{-2}, which corresponds exactly to the ideal average NSLD of the cylinder structure of our asymmetric diblock copolymers. Therefore this part of the film consists of a periodic structure of horizontally oriented deuterated PS cylinders, sandwiched between PBMA layers with a total thickness of this layer of 25 nm. The diameter of the PS cylinders obtained from the fit is 10.6 nm.

However, this morphology does not repeat in the second layer. In contrast, we reveal that a layer with Nb as high as 5.6×10^{-6} Å^{-2} (compare to the Nb of dPS of 6×10^{-6} Å^{-2}) and a thickness of 10.5 nm is formed in the second layer. This bears out the assertion of lamellar PBMA–PS–PS–PBMA morphology for the second layer. We conclude from the slightly reduced value of Nb that the second layer is not complete, resulting in hole formation.

The sample with 5% of nanoparticles shows a similar morphology with a transition from a cylindrical to a lamellar structure. Another remarkable feature is that the nanoparticles with size comparable to the length of the PS domain are incorporated in the PS domains without destroying the structure, just swelling the diameter of the PS cylinders and the thickness of the PS lamellae. Due to this swelling, they become 12.0 nm and 11.7 nm, respectively. The NSLD values reduce in accordance with the values of 2.1×10^{-6} and 5×10^{-6} Å^{-2} for the cylinders and the lamellae.

Upon increasing the volume fraction v_f of the nanoparticles up to 10%, the dimensions of the PS domains, cylinders and lamellae become larger, 15 nm and 13.5 nm, respectively, corroborating that the nanoparticles are incorporated in the structure without destroying it. The corresponding values of NSLD are 2.08×10^{-6} and 4.46×10^{-6} Å^{-2} as obtained from the fit to the data shown in figure 3.

The structure formation of confined films driven by differences in the surface energies of different parts of the copolymer chains was theoretically investigated by Ren *et al* [29].
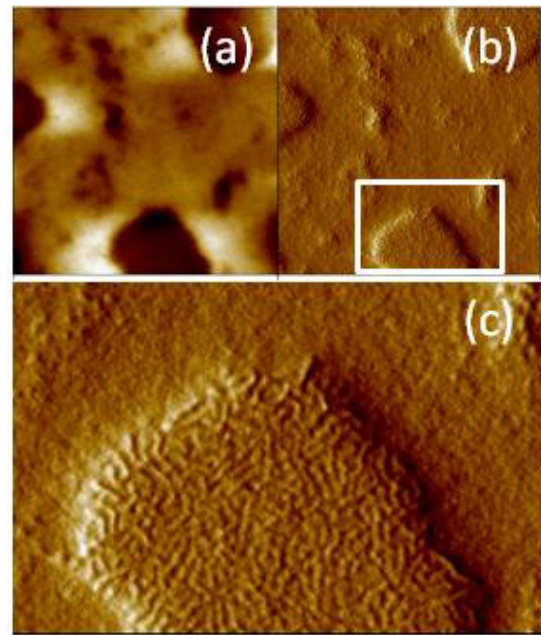

Figure 4. 5 μm $\times$ 5 μm atomic force microscope (AFM) images of the surface of the annealed film of the pure block copolymer P(Sd-*b*-nBMA) measured in tapping mode (a) and phase mode (b). (c) High resolution view of the phase contrast image highlighting the details of the surface of the film, showing the structure with the passage from the bottom cylinder layer to the second lamellar layer. The color scale covers a range from 0 to 30 nm. The zoomed image corresponds to the area marked with the rectangular frame in (b).

Although in this investigation we consider the case of soft confinement where one interface (free surface) is in direct contact with the atmosphere, our studies confirm and allow the further exploitation of the structure transition between cylindrical and lamellar phases.

3.3. Atomic force microscope characterization

The details of the transition from cylindrical to lamellar structure revealed by the neutron reflection experiment are confirmed by AFM measurements. The surface of the films is investigated with the AFM (figure 4). For the example of the annealed pure P(Sd-*b*-nBMA) film we image a representative part of the film surface and visualize details of the cylindrical–lamellar transition by 'looking' inside a hole of the second layer (figure 4(c)). The measurement is performed in phase image mode, because phase imaging highlights edges and is not affected by large-scale height difference. Thus it provides a clearer observation of the fine structures, such as the surface formed by cylinders, with their alignment. In figure 4(c) the bottom of the hole corresponds to the surface of the first layer, clearly showing the horizontally lying cylinders. On the vertical part of the walls, cylinders continuously transform to lamellar forms.

4. Conclusions

We performed a detailed study of a new type of structure of self-assembled composite thin films of asymmetric P(Sd-*b*-nBMA) diblock copolymers and Fe$_3$O$_4$ nanoparticles.

The application of neutron reflectometry in combination with off-specular neutron scattering allows a detailed analysis of the film morphologies. From the neutron reflectometry experiment we obtain quantified information about morphological parameters of the microphase separation structure such as the diameter of the cylinders and the thickness of the lamellae, as well as their modifications due to the incorporation of the nanoparticles. The AFM images of the surface of the first layer in a hole of the second layer visualize and confirm the findings.

We observe in the films investigated mixed cylinder–lamellae morphology and disclose how that structure transformation from cylindrical to lamellar structure happens between the two layers of the thin film. Another remarkable feature is that the big nanoparticles with a size comparable to the length of the PS domain are incorporated in the PS domains without destroying the structure. Instead, the incorporated nanoparticles swell the diameter of the PS cylinders and the thickness of the PS lamellae, resulting in an increased total thickness of the film. The copolymer matrix orders and assembles the nanoparticles into cylindrical–lamellar arrays. Our results show that the composite structure is very stable and that the nanoparticle concentration can reach higher values for these kinds of copolymer films.

Acknowledgments

References

[1] Park S, Lee D H, Xu J, Kim B, Hong S W, Jeong U, Xu T and Russell T P 2009 *Science* **323** 1030
[2] Kim S H, Misner M J, Xu T, Kimura M and Russell T P 2004 *Adv. Mater.* **16** 226
[3] Park S, Wang J-Y, Kim B, Xu J and Russell T P 2008 *ACS Nano* **2** 766
[4] Yoon J, Jin S, Ahn B, Rho Y, Hirai T, Maede R, Hayakawa T, Kim J, Kim K W and Ree M 2008 *Macromolecules* **41** 8778
[5] Bosworth J K, Marvin P Y, Ricardo R, Schwartz E L, Huang J Q, Ko A W, Smilgies D-M, Black C T and Ober C K 2008 *ACS Nano* **2** 1396
[6] Krausch G 1995 *Mater. Sci. Eng.* R **14** 1
[7] Velev O D, Tessier P M, Lenhoff A M and Kaler E W 1999 *Nature* **401** 548
[8] Lambooy P, Russell T P, Kellogg G J, Mayes A M, Gallagher P D and Satija S K 1994 *Phys. Rev. Lett.* **72** 2899–902
[9] Chen X L and Jeneke S A 1998 Quantum confinement effects in thin films of block conjugated copolymer heterostructures *Organic Thin Films* vol 695, ed C W Frank (Washington, DC: ACS) chapter 12, pp 160–77
[10] Suh K Y, Kim Y S and Lee H H 1998 Parallel and vertical morphologies in block copolymers of cylindrical domain *J. Chem. Phys.* **108** 1253–6
[11] Horvat A, Knoll A, Krausch G, Tsarkova L, Lyakhova K S, Sevink G J A, Zvelindovsky A V and Magerle R 2007 *Macromolecules* **40** 6930–9
[12] Karim A, Singh N, Sikka M, Bates F S, Dozier W D and Felcher G P 1994 *J. Chem. Phys.* **100** 1620–9
[13] Schmidt G and Malwitz M M 2003 *Curr. Opin. Colloid Interface Sci.* **8** 103
[14] Balazs A C 2000 *Curr. Opin. Colloid Interface Sci.* **4** 443
[15] Knoll A, Tsarkova L and Krausch G 2007 *Nano Lett.* **7** 843–6
[16] Haes A J and Van Duyne R P A 2002 *J. Am. Chem. Soc.* **124** 10596–604
[17] Arico A S, Bruce B, Scrosati B, Tarascon J M and van Schalkwijk W 2005 *Nat. Mater.* **4** 366–77
[18] Maier S A, Kik P G, Atwater H A, Melzter S, Harel E, Koel B E and Requicha A A G 2003 *Nat. Mater.* **2** 229–32
[19] Lauter-Pasyuk V, Lauter H J, Ausserre D, Gallot Y, Cabuil V, Hamdoun B and Kornilov E I 1998 *Physica* B **248** 243
[20] Lauter-Pasyuk V, Lauter H J, Ausserr D, Gallot Y, Cabuil V, Kornilov E I and Hamdoun B 1998 *Physica* B **241–243** 1092
[21] Lefebure S, Cabuil V, Ausserre D, Paris F, Gallot Y and Lauter-Pasyuk V 1998 *Prog. Colloid Polym. Sci.* **110** 94
[22] Leibler L 1980 *Macromolecules* **13** 1602
[23] Khandpur A K, Forster S, Bates F S, Hamley I W, Ryan A J, Bras W, Almdal K and Mortensen K 1995 *Macromolecules* **28** 8796
[24] Anastasiadis S H, Russel T P, Satija S K and Majkrzak C F 1989 *Phys. Rev. Lett.* **62** 1852
[25] Lauter-Pasyuk V, Lauter H J, Gordeev G P, Mueller-Buschbaum P, Toperverg B P, Jernenkov M and Petry W 2003 *Langmuir* **19** 7783–8
[26] Matsen M W and Bates F S 1997 *J. Polym. Sci. Pol. Phys.* **35** 945
[27] Zhang X, Berry B C, Yager K G, Kim S, Jones R L, Satija S, Pickel D L, Douglas J F and Karim A 2008 *ACS Nano* **2** 2331–41
[28] Peinemann K-V, Abetz V and Simon P F W 2007 *Nat. Mater.* **6** 992
[29] Ren C-L, Chen K and Ma Yu-Q 2005 *J. Chem. Phys.* **122** 154904
[30] Bockstaller M R, Lapetnikov Y, Margel S and Thomas E L J 2003 *Am. Chem. Soc.* **125** 5276–7
[31] Matsen M W and Thompson R B 2008 *Macromolecules* **41** 1853–60
[32] Pyun J 2007 *Polym. Rev.* **47** 231
[33] Balazs A C, Emrick T and Russell T P 2006 *Science* **314** 1107
[34] Sanchez C, Julian B, Belleville P and Popall M 2005 *J. Mater. Chem.* **15** 3559
[35] Abul Kashem M M, Perlich J, Schulz L, Roth S V, Petry W and Müller-Buschbaum P 2007 *Macromolecules* **40** 5075
[36] Xu C, Ohno K, Ladmiral V, Milkie D, Kikkawa J M and Composto R J 2009 *Macromolecules* **42** 1219–28
[37] Park M L and Char K 2006 *Langmuir* **22** 1375–8
[38] Müller-Buschbaum P 2003 *Eur. Phys. J.* E **12** 443
[39] Lauter V, Ambaye H, Goyette R, Lee W T H and Parizzi A 2009 *Physica* B **404** 2543
[40] Spectrometer of polarized neutrons http://flnp.jinr.ru/139/
[41] Penfold J and Thomas R K 1990 *J. Phys.: Condens. Matter* **2** 1369–412
[42] Lauter-Pasyuk V, Lauter H J, Toperverg B P, Petrenko A, Schubert D, Schreiber J, Burcin M and Aksenov V 2002 *Appl. Phys.* A **74** S528–30